**Geomechanics and Engineering**, *Vol. 42, No. 4 (2025) 309-320*
https://doi.org/10.12989/gae.2025.42.4.309


# Study on the effects of double-pipe grouting in silt-sand composite strata on surrounding soil and bridge substructures

Zhijie Peng[a], Tingjin Liu*, Liangyi Cai[b], Huashan Zhong[c] and Jitao Jia[d]

*School of Civil Engineering and Transportation, South China University of Technology, Guangzhou 510640, Guangdong, China*

(*Received December 25, 2024, Revised July 30, 2025, Accepted August 7, 2025*)

**Abstract.** This study proposed a new "grouting-soil-pier interaction transmission model", using work done on soil per linear meter to reflect the impact of soil displacement on the bridge pier. Exploring the relationship between grouting volume, soil displacement, and bridge pier displacement, the relationship between bridge pier horizontal displacement and grouting volume is divided into three zones: linear, nonlinear, and ineffective. A continuous transition from linear to nonlinear behavior is formulated, thereby elucidating the entire progression of pier displacement. For the present project, In the range of grouting distance [0, 5] meters and volume [0, 120] cubic meters, a proportional relationship is observed. Field tests show that the error between derived and measured slopes of pier displacement is under 10%, validating the model. Further exploration reveals that the maximum bending moment and maximum soil displacement occur at the same depth, which corresponds to the silt layer. Under different pile deflection conditions, the ratio of work done on soil per linear meter to pile strain energy varies, indicating different energy transfer efficiencies.

**Keywords:** bridge pier displacement; empirical model; micro-disturbance grouting; silt-sand composite strata; soil lateral displacement

## 1. Introduction

Grouting construction can significantly impact the surrounding soil and existing structures, potentially causing ground heave or soil lateral displacement, with lateral displacement being particularly pronounced in soft soil strata. Elevated bridges have become widely used in urban rapid transit systems, highlighting the importance of protecting bridge piles. In southern coastal regions of China, where soft clay predominates with high sensitivity and compressibility, grouting near construction sites causes more pronounced disturbances to the soil compared to other strata. New construction activities can affect existing structures, inducing displacement and deformation (Boschi *et al.* 2020, Ma *et al*. 2024), thus necessitating preventive or remedial measures.

Preventive measures typically involve the use of high-pressure jet grouting technology to create isolation walls (Bayesteh and Sabermahani 2020, Zhang *et al*. 2020) or ground reinforcement (Sha *et al.* 2024, Wang *et al*. 2021). Remedial methods primarily involve grouting to correct displacement and deformation of bridge piers after they occur (Fu *et al*. 2023,; Park and Oh 2018). Whether for prevention or remediation, the grouting process can damage existing structures (Shan *et al*. 2024, Wang *et al*. 2019, Wu *et al.* 2016). Grouting treatment is widely applied in engineering, with particular attention paid to its effects on nearby bridge substructures and soil displacement patterns, which is the focus of this study.

Over the past few decades, numerous scholars have conducted extensive research on jet grouting (Cheng *et al*. 2023, Flora *et al.* 2013, Kim *et al*. 2024). In engineering applications, jet grouting technology can be classified into three types based on the injection method: (a) single-pipe grouting system, (b) double-pipe grouting system, and (c) triple-pipe grouting system. The triple-pipe system, also known as high-pressure jet grouting (water + slurry + air), has become increasingly prevalent in recent years. Jet grouting essentially compresses the soil strata, inevitably causing lateral displacement of soil and even surface upheaval. Theoretical studies (CAO 2001; El-Kelesh *et al*. 2001) proposed models for cavity diffusion in clay under undrained conditions. Shen et al. and Fu *et al*. (2017) suggested semi-theoretical methods for predicting surface displacement under vertical grouting. Liu *et al*. (2017) proposed a theoretical model for high-pressure grouting in soft soils to study its effects, which they validated through field measurements. Li *et al*. (2024) analyzed cavity expansion based on strength criteria and energy theory.

To date, most studies have focused on the disturbance caused by high-pressure jet grouting (triple-pipe system) to both the internal and surface layers of the soil. However, due to the complexity of grouting parameters, uncertain grout discharge, and varying soil compositions, the applicability of these research findings is often highly limited. In comparison to the triple-pipe system, the double-pipe grouting system does not discharge grout, making

*Corresponding author, Professor
E-mail: liutj@scut.edu.cn
[a]Master Student
[b]Ph.D. Student
[c]Ph.D. Student
[d]Master Student



ISSN: 2005-307X (Print), 2092-6219 (Online)

Table 1 In-situ soil sample parameters

| Items | Miscellaneous fill | Silt | Silty clay | Medium coarse sand |
|---|---|---|---|---|
| Water content (w/%) | 22.8 | 47.6 | 24.3 | – |
| Density ($\rho$/(g/cm3)) | 2.03 | 1.65 | 2.00 | 1.9 |
| Dry density ($\rho_d$/(g/cm3)) | 1.65 | 1.12 | 1.61 | – |
| Degree of saturation ($S_r$/%)) | 97.2 | 92.8 | 97.3 | – |
| Void ratio ($e_0$) | 0.633 | 1.344 | 0.672 | – |
| Coefficient of compressibility ($a_{1\text{-}2}$/(MPa-1)) | 0.3 | 13.3 | 0.31 | – |
| Modulus of compressibility ($Es_{1\text{-}2}$/(MPa)) | 5.4 | 2.20 | 5.40 | 20 |
| Cohesion ($c$/kPa) | 12 | 6.8(UU) | 11 | – |
| Angle of internal friction ($\varphi$/°) | 7 | 6.0(UU) | 10 | 32 |
| Poisson's ratio ($\mu$) | 0.35 | 0.44 | 0.35 | 0.4 |

research on grouting with discharge conditions less applicable in this context. A few studies have explored the effects of micro-disturbance double-pipe grouting on tunnel uplift (Lu *et al.* 2024) and lateral displacement correction (Zhang *et al.* 2024), or used numerical methods to investigate the effects of horizontal grouting beside the tunnel (Ma *et al.* 2024, Wang and Zheng 2024). However, the primary focus of these studies has been on the corrective effects of grouting on tunnel alignment, with insufficient attention paid to the resulting soil displacements. Shan *et al.* (2024) studied the relationship between the influence distance and depth of triple-pipe grouting in soft soil, while Li *et al.* (2025) investigated soil displacement and bridge pile response under lateral overloading of piles in soft soil, as well as the widespread use of inclinometers (Jia *et al.* 2023, Milkevych *et al.* 2018, Sun *et al.* 2014) to monitor deep soil lateral displacement in engineering. While these studies focus on soil displacement and bridge movement, they treat them as independent phenomena without examining the interrelationship between them. As a result, the interaction among grouting, soil, and bridge structures remains insufficiently explained, and a comprehensive quantitative analysis of their coupled behavior is notably absent.

This paper proposes a novel and simplified method that utilizes the work done on soil per linear meter as a medium to explore the relationship between grouting volume, soil displacement, and bridge pier displacement. The proposed method fully incorporates the influence of soil displacement across the entire depth range. Furthermore, it elucidates the nonlinear evolution of bridge displacement and soil movement throughout the grouting process, thereby capturing the full progression of their interaction. Several field measurement cases are presented to validate the effectiveness of this method, and further exploration of potential pile deflection scenarios and their associated strain energy is conducted.

## 2. Preparation for field measurements

### 2.1 Soil properties

Field in-situ tests and laboratory tests were conducted as part of the investigation. The vane shear tests were performed on-site, while laboratory tests included measurements of the soil sample's water content, density, compression modulus, internal friction angle, and cohesion. The remaining parameters were sourced from the geological survey report. The grading curve for the medium-coarse sand layer is presented in Fig. 1, and the results of the vane shear tests are shown in Fig. 2. The sensitivity of the silty soil was found to range from 1.9 to 3.0.

### 2.2 Monitoring plan

To investigate the impact of micro-disturbance grouting on soil displacement and bridge pier displacement in composite strata, relying on field construction, the lateral displacement of soil and the horizontal displacement and settlement of the bridge pier were monitored during the construction process. Horizontal displacement of the deep

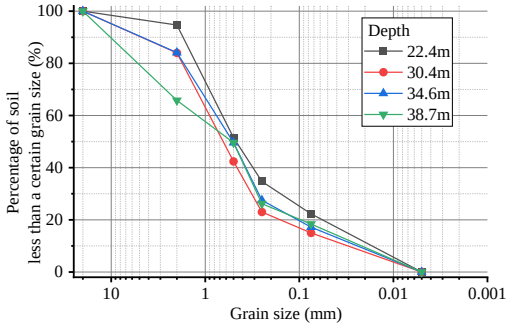


Fig. 1 Gradation curve of the medium coarse sand

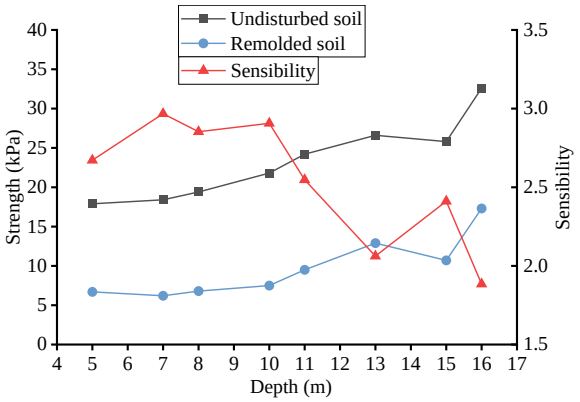


Fig. 2 Results of the vane shear test in silt layers

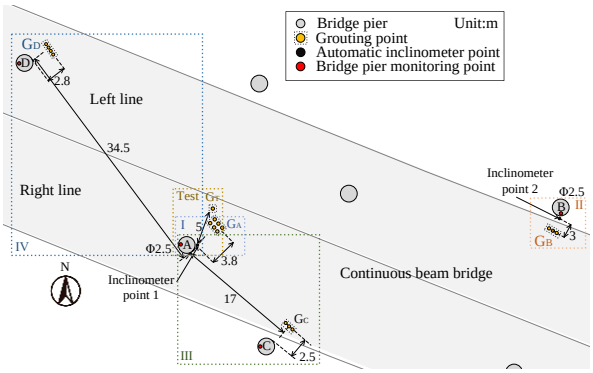


Fig. 3 Schematic diagram of monitoring points

soil was measured using automated inclinometers, which provide superior sampling frequency, accuracy, and efficiency compared to manual inclinometers. The sensor spacing was set at 1 meter, with an accuracy of 0.005 mm per 500 mm. The device utilized an embedded MEMS triaxial accelerometer to collect gravity acceleration data along different axes, and displacement was calculated based on changes in angle, assuming a fixed segment length.

Inclinometer 1 was installed on the east side of bridge pier A, at a distance of 0.2 meters from the pier. Inclinometer 2 was installed on the south side of bridge pier B, also at an approximate distance of 0.2 meters. A schematic of the monitoring points is shown in Fig. 3. A total of five grouting points were monitored, with data from four points ($G_T$, $G_A$, $G_C$, $G_D$) collected by Inclinometer 1, and data from one point ($G_B$) collected by Inclinometer 2.

Horizontal displacement and settlement of the bridge piers were monitored manually using a Leica TS60 total station for data collection. The angular accuracy of the total station is 0.5", and its distance accuracy is 0.6 mm + 1 ppm.

### *2.3 Grouting plan*

This project employs a micro-disturbance double-pipe grouting method. Liquid A is sodium silicate (water glass), and Liquid B is cement slurry, which are mixed in a certain proportion (see construction parameters in Table 2). The reinforcement principle is that the mixed liquid is injected into the soil layers, forcing the water between the soil

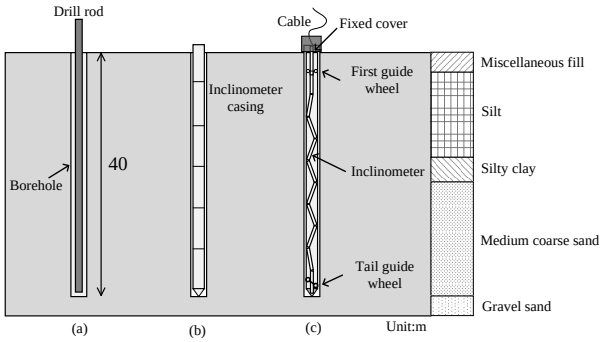


Fig. 1 Installation process of inclinometer

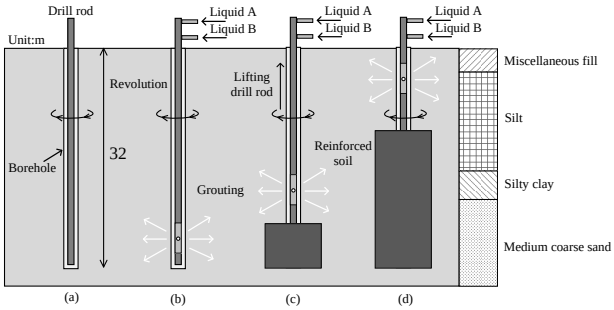


Fig. 5 Schematics of micro disturbance dual-pipe grouting

Table 2 The grouting parameters of this project

| Grouting parameters | Value |
|---|---|
| Grouting pressure (MPa) | 1.5 |
| Water-cement ratio (mass ratio) | 1:1 |
| Water glass to cement slurry ratio (volume ratio) | 1:1 |
| Initial setting time of the mixed liquid (s) | 45~55 |
| Grouting depth (m) | 17&32 |

particles to be expelled. This fills the voids with the slurry and consolidates the soil, thereby achieving reinforcement.

The specific process of double-pipe grouting is summarized in the following three steps (refer to Fig. 5): Step 1. Determine the grouting hole location, drill the hole, lower the grouting pipe to the desired depth, and connect the grouting system. Step 2. Begin grouting, slowly raise the grouting pipe when the set pressure is reached, and continue raising until the grouting is complete. Step 3. Complete the grouting and seal the hole.

Unlike other high-pressure jet grouting methods, the micro-disturbance grouting method does not have a fixed pipe lifting time (high-pressure jet grouting typically raises the drill rod by a fixed step length). The lifting of the pipe is based on whether the set grouting pressure has been reached. Additionally, this method does not discharge slurry, whereas high-pressure jet grouting may experience some slurry backflow (Cheng *et al*. 2023, Shen *et al.* 2017, Wang *et al*. 2019).

The grouting conditions in this study are divided into five groups, as shown in Table 3: the Test Group, Group I, Group II, Group III, and Group IV. The conditions are

Table 3 Grouting and monitoring point arrangement for each group

| Group | Grouting position | Distance (m) | Duration (Day) | The inclinometer used | Monitoring piers |
|---|---|---|---|---|---|
| Test group | $G_T$ | 5 | 1 | Inclinometer 1 | Pier A |
| Group I | $G_A$ | 3.8 | 6 | Inclinometer 1 | Pier A |
| Group II | $G_B$ | 3 | 3 | Inclinometer 2 | Pier B |
| Group III | $G_C$ | 17&2.5 | 3 | Inclinometer 1 | Pier A&Pier C |
| Group IV | $G_D$ | 34.5&2.8 | 4 | Inclinometer 1 | Pier A&Pier D |

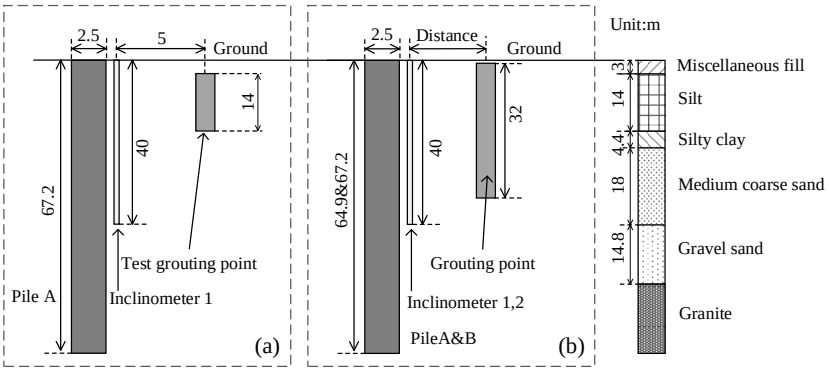


Fig. 2 Profile of the groups: (a) Test group and (b) Group I~IV

named in the order of construction, with no overlap in time between each condition. A schematic layout of the conditions is provided in Fig. 6.

## 3. Analysis of results

### *3.1 Single grouting test*

In order to determine the relevant parameters during the grouting process (such as the distance between the bridge pier and the grouting point, grouting volume, grouting pressure, etc.), a single grouting test was conducted. The grouting pressure was set at approximately 1.5 MPa based on engineering experience, and thus, the influence of different grouting pressures is not explored in this study. The grouting was mainly applied to the silt layer (with a depth range of 3 to 17 meters), and a total of 7.8 m³ of mixed grout was injected. The horizontal distance between the grouting point $G_T$ and the inclinometer 1 is 5 meters, and the distance between inclinometer 1 and bridge pier A is 0.2 meters (see Fig. 6(a)).

During the grouting process, the lateral displacement of the soil exhibited a significant variation from bottom to top, with the displacement curve showing a bell-shaped distribution - larger in the middle and smaller at both ends (see Fig. 7). The maximum displacement value was 36.64 mm, which occurred at a depth of 10 meters. The sand and silty clay layers, where no grouting was performed, exhibited negligible lateral displacement.

To establish the relationship between the lateral displacement of the soil and the horizontal displacement of the bridge, the study investigates the work done on the soil per linear meter and its impact on the horizontal

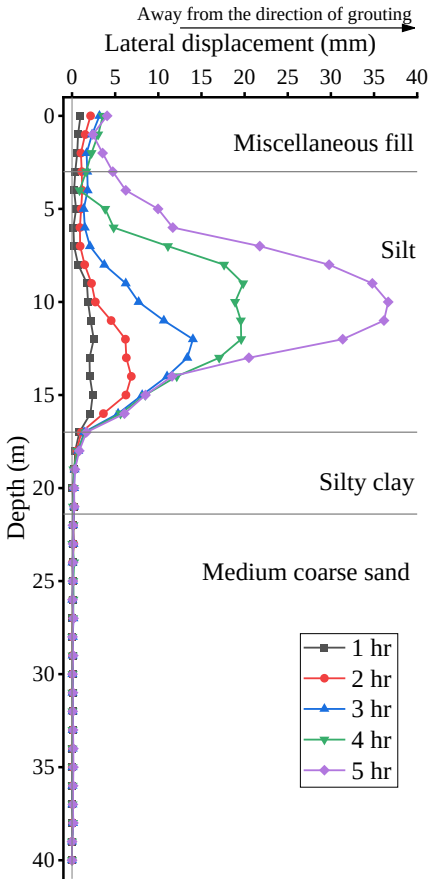


Fig. 7 Lateral displacement of soil in the test group

displacement of the pier. Taking the soil between the inclinometer and the bridge pier as an example, the lateral displacement of the soil can be regarded as compression of

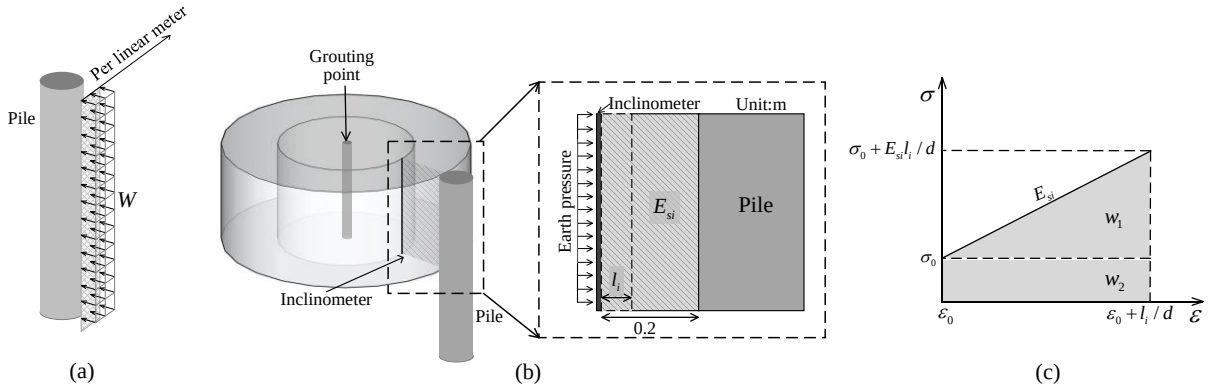


Fig. 8 Schematic diagram of work calculation: (a) distribution of work done per linear meter, (b) strain calculation and (c) loading curve

the soil mass. Assuming the soil behaves as a linear elastic material, the strain of the soil is calculated using the method shown in Fig. 8. The stress increment acting on the soil is then determined using the Young's modulus formula. By incorporating the at-rest earth pressure, the total work done on the soil per linear meter can be computed.

In this study, the length of the bridge pier exceeds that of the inclinometer tube, but the bottom of the inclinometer is located in a medium-coarse sand layer, and the lateral displacement curve tends to converge to zero with increasing depth. Therefore, it is assumed that the lateral displacement of the soil below a depth of 40 meters is zero.

The formulae are as follows

$$\sigma_i = E_{si} \Delta\varepsilon_i \tag{1}$$

$$\Delta\varepsilon_i = \frac{l_i}{d} \tag{2}$$

$$W = \sum_{i=1}^{L} \sigma l_i * 1 \tag{3}$$

$$W_1 = \frac{\sum_{i=1}^{L} E_{si} l_i^2 * 1}{2d} \tag{4}$$

$$W_2 = \sum_{i=1}^{L} \sigma_0 l_i * 1 \tag{5}$$

$$W_t = W_1 + W_2 \tag{6}$$

$$\sigma_0 = \gamma z K_0 \tag{7}$$

$$K_0 = 1 - \sin\varphi' \tag{8}$$

Where: $\sigma_i$ is the additional earth pressure; $E_{si}$ is the compressive modulus of the soil at depth $i$; $\Delta\varepsilon_i$ is the additional strain; $l_i$ is the lateral displacement of the soil at depth $z$ (with a sensor spacing of 1 meter); $d$ is the distance

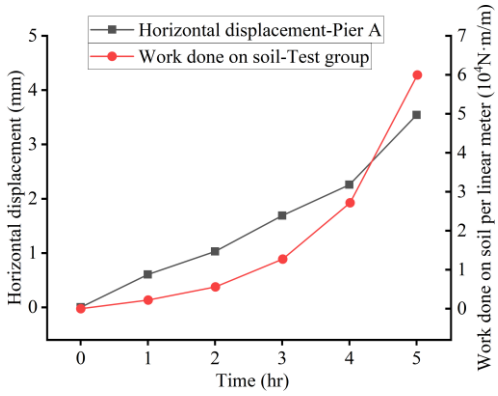


Fig. 9 Horizontal displacement of pier A and work done on soil per linear meter

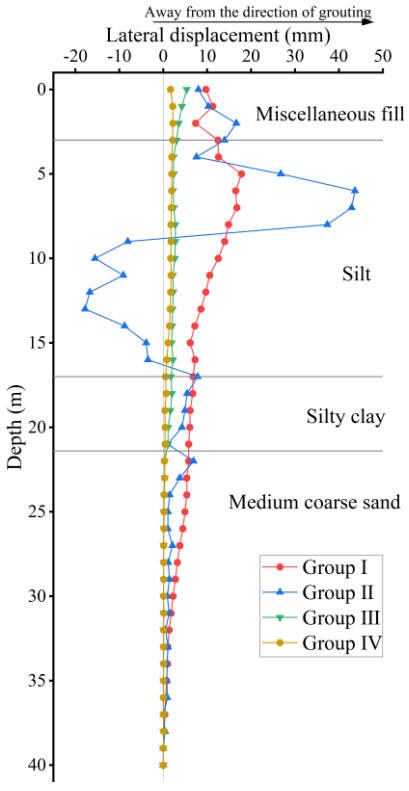


Fig. 10 Lateral displacement of soil for group I to IV

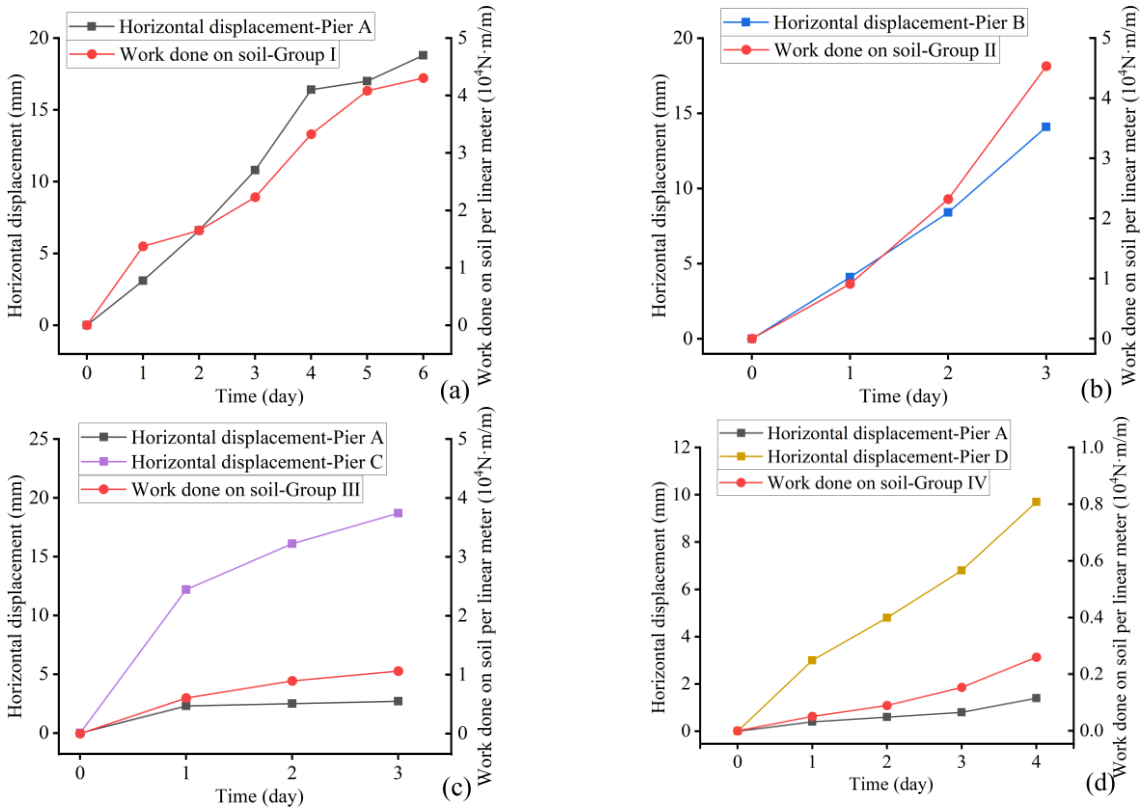


Fig. 3 Horizontal displacement of bridge piers and work done on soil per linear meter: (a) Group I, (b) Group II, (c) Group III and (d) Group IV

between the inclinometer and the bridge pier; $W$ is the work done on soil per linear meter (in the direction perpendicular to the pile); $W_1$ is the work done on soil per linear meter by the additional earth pressure; $W_2$ is the work done on soil per linear meter by the at-rest earth pressure; $L$ is the pile length; $W_t$ is the total work done on soil per linear meter by the total earth pressure; $\sigma_0$ is the at-rest earth pressure; $\gamma$ is the unit weight of the soil; $z$ is the depth of the calculation point; $K_0$ is the coefficient of at-rest earth pressure, calculated using the empirical formula (Jaky 1944); $\varphi'$ is the effective internal friction angle of the soil.

When comparing the work done on soil per linear meter with the horizontal displacement of bridge pier A (as shown in Fig. 9), it can be observed that both increase simultaneously during the grouting process, with the rate of growth accelerating over time.

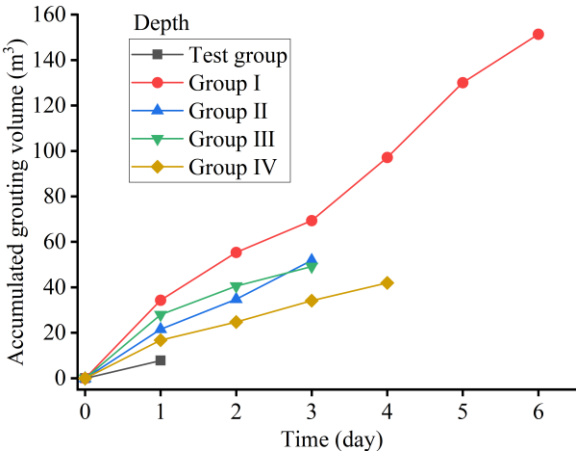


Fig. 12 Accumulated grouting volume

### 3.2 Multiple grouting groups

A total of four groups of multiple grouting field tests were conducted, with the grouting volume shown in Fig. 12. For Group I, significant displacement initially occurred in the silt layer, followed by displacement development in the sand layer. This sequence is attributed to the specific characteristics of the grouting method used (dual-pipe grouting). Unlike the commonly used high-pressure jet grouting method, this method does not discharge grout. Instead, it first fills the voids in the sandy soil during grouting, which results in minimal displacement of the sand layer in the early stages. In the later stages of grouting, the grout solidified within the voids of the sand layer, forming an impermeable reinforcement body. Continued grouting then pushed this reinforcement body outward.

For Group II, the lateral soil displacement exhibited an S-shaped pattern, with the maximum displacement still occurring within the silt layer, moving away from the grouting point. For Group III (at a distance of 17 m) and Group IV (at a distance of 34.5 m), the response of the strata was weaker due to the increased distance from the inclinometer. For all multiple grouting groups, the work done on the soil per linear meter and the horizontal displacement of the bridge pier progressed in a coordinated manner, both showing an upward trend.

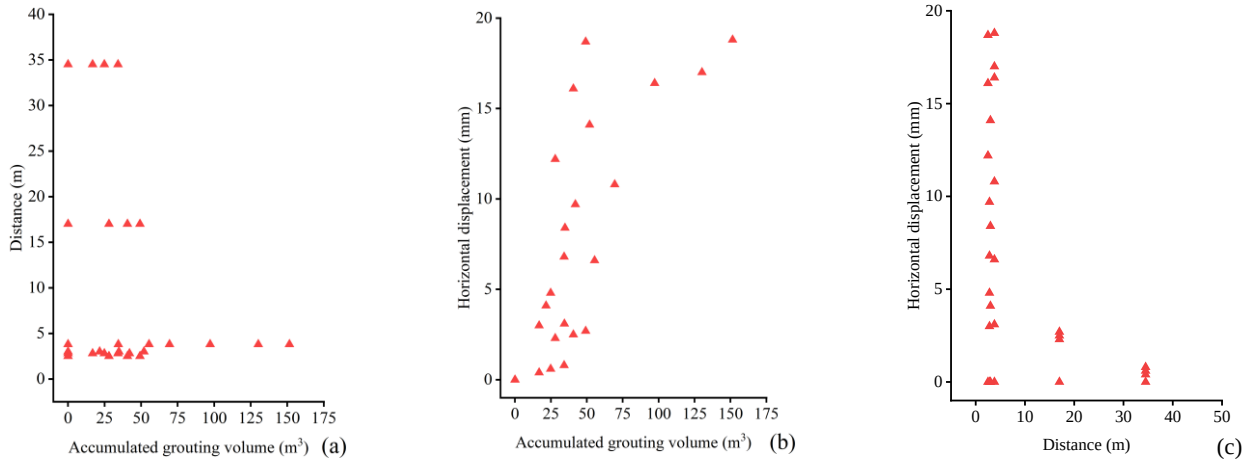


Fig. 13 Scatter plots of accumulated grouting volume, distance, and horizontal displacement

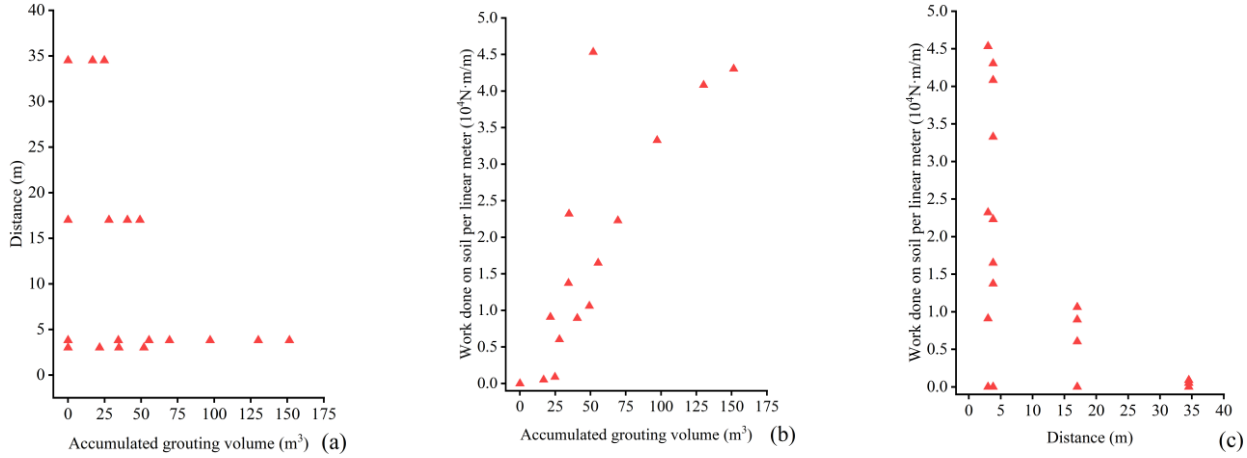


Fig. 14 Scatter plots of grouting volume, distance, and work done on soil per linear meter

### *3.3 Summary*

During the field measurement phase, five sets of grouting operations were performed. Both the horizontal displacement of the bridge pier and the work done on soil per linear meter exhibited a decreasing trend with increasing grouting distance (see Figs. 13 and 14), while both parameters increased as grouting volume increased. Based on the data obtained from the field tests, three-dimensional surface and contour plots were created to illustrate the relationship between grouting volume, distance, and the horizontal displacement of the bridge pier. Additionally, the Poly2D function was applied for surface fitting, and the fitted three-dimensional surface and contour plots were generated (Fig. 15). In these plots, the X and Y axes represent the accumulated grouting volume and the distance between the grouting point and the bridge pier, respectively, while the Z axis represents the horizontal displacement of the bridge pier.

The Poly2D surface fitting function used is shown in Eq. (9)

$$z = z_0 + ax + by + cx^2 + dy^2 + fxy \tag{9}$$

The measured and fitted data both indicate that, for a given grouting distance, the horizontal displacement of the bridge pier gradually decreases as the grouting volume increases. Due to the limited field grouting data, an extrapolation was made using the fitting method, assuming that each grouting distance corresponds to a maximum horizontal displacement of the bridge pier.

In Fig. 16, the black dashed line represents the maximum horizontal displacement of the bridge pier at a given distance. The area enclosed by this line and the X/Y axes is considered the effective grouting zone. The red dashed line marks the boundary where the relationship between grouting volume and horizontal displacement transitions from linear to nonlinear. The area enclosed by this line and the X/Y axes is regarded as the linear zone. Therefore, the relationship between grouting volume and horizontal displacement is divided into three regions: the linear zone, the nonlinear zone, and the ineffective zone.

The drawing of the black line is based on the line connecting the intersection points of the horizontal line and the contour lines. The engineering implication of this line is that beyond this point, further increases in grouting volume will not result in a corresponding increase in horizontal displacement. The drawing of the red line is based on the

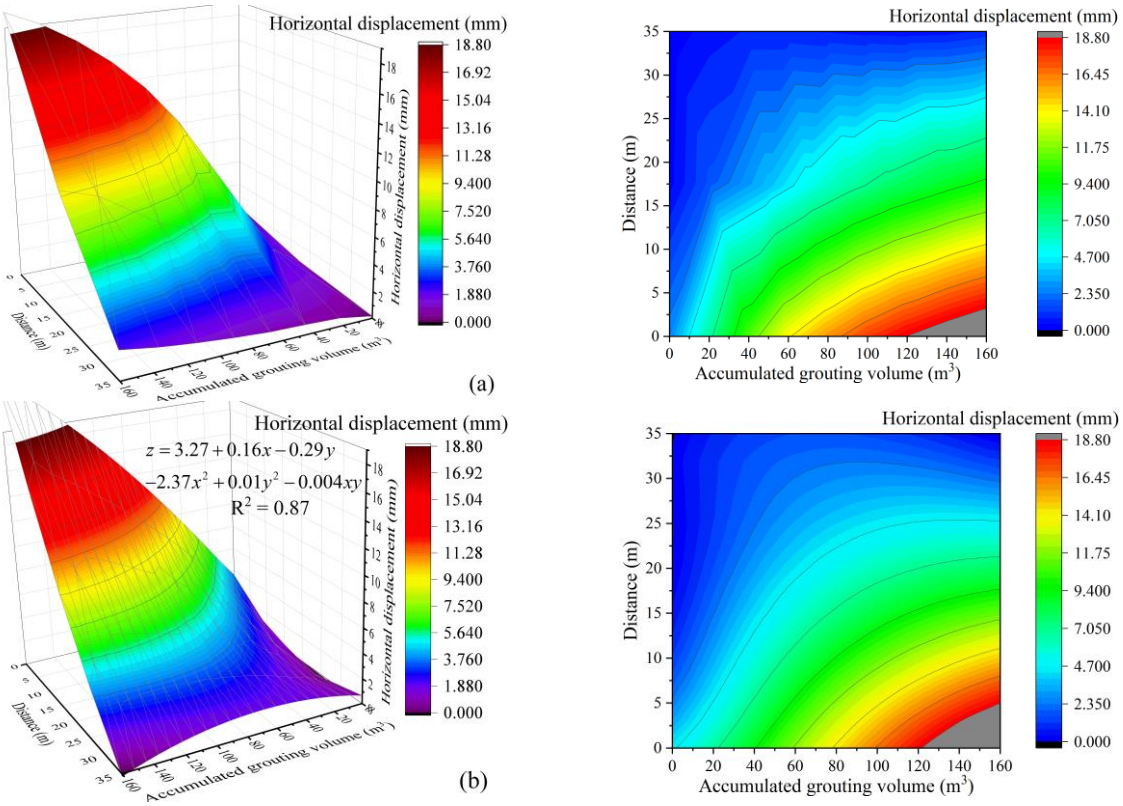


Fig. 15 Surface and contour plot of horizontal displacement of bridge piers: (a) raw data and (b) Fitted data

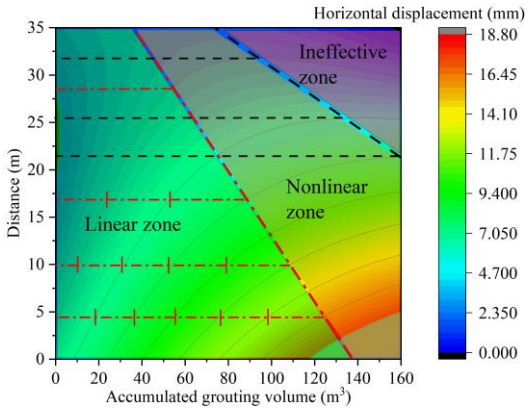


Fig. 16 Schematic diagram of the relationship between grouting volume, distance, and horizontal displacement

fact that the horizontal displacement change between adjacent contour lines is determined. If the ratio of grouting change to initial change at a certain point is 1.5, it can be approximated as the boundary where the relationship between grouting volume and horizontal displacement transitions from linear to nonlinear.

In this study, considering the grouting and geological conditions, with grouting distances ranging from 0 to 5 meters and grouting volumes between 0 and 120 m³, the horizontal displacement of the bridge pier can be considered directly proportional to the accumulated grouting volume. In practical engineering applications, the grouting distance should be determined based on economic considerations and the need to minimize disturbance to the surrounding environment.

## 4. Discussions

### *4.1 Grouting-soil-pier interaction transmission model*

There is a defined relationship between the grouting volume, the work done on soil per linear meter, and the horizontal displacement of the bridge pier. Within the previously mentioned linear zone, the grouting volume and the horizontal displacement of the bridge pier exhibit a linear relationship. Based on the observed data trends, a "grouting-soil-pier interaction transmission model" is proposed, with energy acting as the medium. This model assumes linear relationships between the grouting volume, the work done on soil per linear meter, and the horizontal displacement of the bridge pier, which will be discussed in detail later. A schematic representation of the model is shown in Fig. 17.

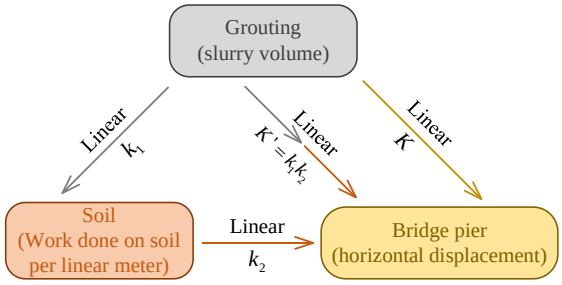


Fig. 17 Schematic diagram of the model

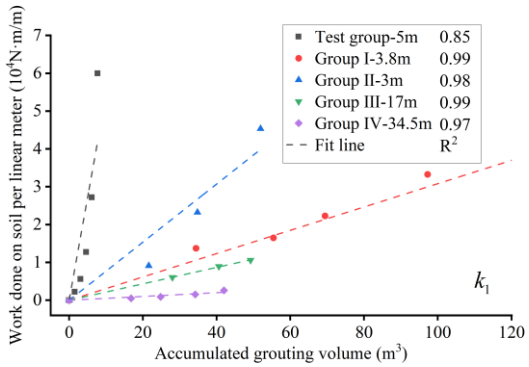


Fig. 18 The function of work done on soil per linear meter with respect to accumulated grouting volume

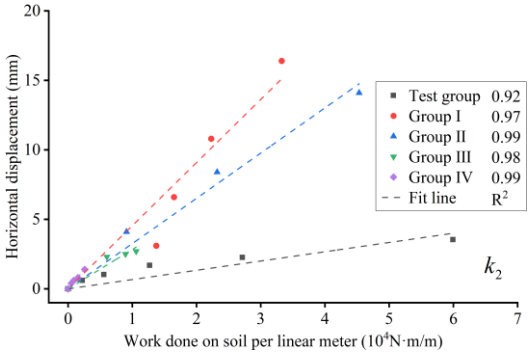


Fig. 19 The function of horizontal displacement of bridge piers with respect to work done on soil per linear meter

The scatter plots for the points within the linear zone are shown in Figs. 18-20. For each group within the same plot, linear fitting methods were applied (as shown in Table 4). The expressions for the fitted lines are as follows

$$W_t = k_1 V \tag{10}$$

$$D_H = k_2 W_t \tag{11}$$

$$D_H = KV \tag{12}$$

$$K' = k_1 k_2 \tag{13}$$

Where: $W_t$ is the work done on soil per linear meter, $k_1$ is the slope of the fitted line for the relationship between work done on soil per linear meter and accumulated grouting volume, $V$ is the accumulated grouting volume, $D_H$ is the horizontal displacement of the bridge pier, $k_2$ is the slope of the fitted line for the relationship between horizontal displacement and work done on soil per linear meter, $K$ is the slope of the fitted line for the relationship between horizontal displacement and accumulated grouting volume, $K'$ is the derived slope of $K$.

$k_1$ represents the influence of grouting on the surrounding soil. With the exception of the test group, the slopes $k_1$ for the other groups decrease as the grouting distance increases (see Fig. 18). In the test group, the grouting depth is within the silt layer, and due to the high sensitivity of the silt soil, significant soil displacement occurred during the grouting process. As a result, some of the soil may have bypassed the bridge pier (Li *et al.* 2025), leading to an overestimation of the work done on soil per linear meter.

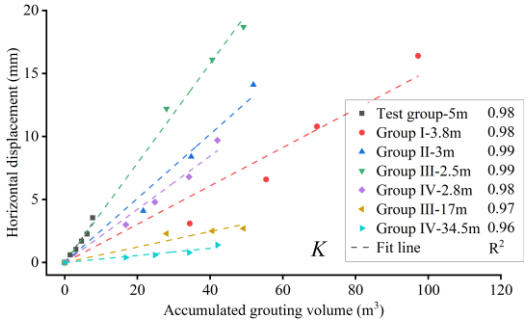


Fig. 20 The function of horizontal displacement of bridge piers with respect to accumulated grouting volume

$k_2$ represents the extent to which the work done on soil per linear meter affects the horizontal displacement of the bridge pier. For the same horizontal displacement of the bridge pier, the work done on soil per linear meter varies (see Fig. 19). For groups with the same grouting depth (Groups I to IV), the slopes $k_2$ are similar, with the exception of the test group, which has a lower slope. This could be due to differences in grouting depth.

The results indicate that for groups with the same grouting depth (Groups I to IV), the values of $K'$ and $K$ exhibit relatively small error rate, with the overall error rate being less than 10%. However, the test group shows a larger error, which is likely due to some of the silt soil bypassing the bridge pier. As a result, for the test group, the work done on soil per linear meter does not adequately reflect the transmission process. The absence of certain data in Table 4 is mainly due to the lack of inclinometer installation on the respective sides of the bridge piers, thereby preventing the acquisition of the corresponding derived values.

For the groups with the same grouting depth (Groups I to IV), the corresponding slopes $K$ and grouting distance $D$ are fitted using a hyperbolic function. The expression is as follows

$$K = \frac{P_1 D}{P_2 + D} \tag{14}$$

Where: $P_1$ and $P_2$ are the coefficients, which need to be obtained by fitting the actual measured data.

A "grouting-soil-pier interaction transmission model" was established using the work done per linear meter of the soil as an intermediate variable. The derived $K'$ is found to be close to the measured $K$, with the overall error rate being less than 10%. This indicates that the work done on soil per linear meter can effectively reflect the relationship between the grouting process and the bridge pier, thus proving the validity of the model. While the method has demonstrated validity within the specific geological context of this project, further studies are required to assess its generalizability to a broader range of geological conditions.

As shown in Fig. 20, for the same grouting volume, different grouting distances result in different horizontal displacements of the bridge pier. The fitting results (Fig. 21)

Table 1 Linear fitting parameters

| Group | $k_1$ | $k_2$ | $K'$ | K | Error rate |
|---|---|---|---|---|---|
| Test Group-5 m | 5430.3 | 6.7E-5 | 0.364 | 0.407 | 10.6% |
| Group I-3.8 m | 308.3 | 4.5E-4 | 0.139 | 0.152 | 8.73% |
| Group II-3 m | 767.9 | 3.3E-4 | 0.253 | 0.255 | 0.62% |
| Group III-2.5 m | – | – | – | 0.395 | – |
| Group IV-2.8 m | – | – | – | 0.211 | – |
| Group III-17 m | 217.2 | 2.8E-4 | 0.061 | 0.062 | 1.91% |
| Group IV-34.5 m | 50.2 | 5.5E-4 | 0.028 | 0.028 | 1.39% |

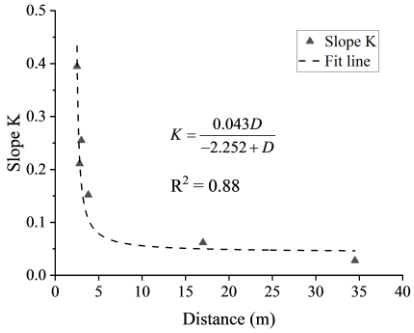


Fig. 21 Curve fitting between slope $K$ and distance $D$

can be applied to projects with similar geological formations. For experimental grouting in projects, where sufficient data to derive the relationship between horizontal displacement of the bridge pier and grouting volume are unavailable, the relationship between work done on soil per linear meter and horizontal displacement of the bridge pier can be calculated using inclinometer data (i.e., obtaining $k_2$). This provides real-time feedback for the construction process.

### 4.2 Pile strain energy

The measured data indicates that, under similar grouting conditions, the displacement behavior of deep soil layers varies. Soil displacement provides a general indication of changes in pile deflection. Li *et al*. (2025) conducted a field study on the lateral overloading of bridge piers in soft soil layers for high-speed railway bridges, finding that the deflection of the bridge pier was approximately 0.5 times the lateral displacement of the surrounding soil. Zhao and Wang (2018) applied the compressive sampling (CS) method to process raw discrete measurement data of bridge pier deflection, enabling the accurate derivation of the nearly continuous lateral response of the bridge pier, including bending moments and shear forces.

Based on the measured data, various potential deflection curve scenarios for the pile foundation were plotted (Fig. 22). For each scenario, the deep soil displacement corresponding to the same horizontal displacement of the bridge pier was extracted and transformed. The bending moment for each scenario was calculated, and the pile strain energy was determined using Eq. (15) (Fig. 23). Since the bottom of the inclinometer is situated within a stable sand layer and the data from depths of 30-40 meters tend to

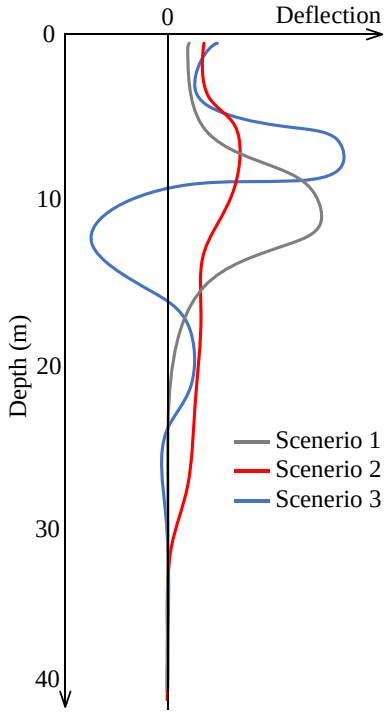


Fig. 22 Schematic diagram of pile deflection in various scenarios

stabilize at zero, it is assumed that the deflection of the bridge pier from the inclinometer bottom to the pier base is zero.

$$U = \frac{1}{2}\int_0^L \frac{M^2}{EI}dx \tag{15}$$

Where: $U$ is strain energy, $L$ is pile length, $M$ is transverse bending moment, $I$ is area moment of inertia, the Young's modulus, $E$, is taken as 31.5 GPa according to recommendations in Code for Design of Concrete Structures (2010, China).

The results indicate that under grouting conditions, lateral displacement in the silt layer is more pronounced than in the sand layer, exerting greater additional earth pressure on the bridge pile. Consequently, the maximum bending moment occurs at the corresponding depth within the silt layer, aligning with the point of maximum lateral soil displacement. This effect is primarily concentrated in the silt layer, while the bending moment is notably smaller in the silty clay and sand layers, Xia *et al*. (2024) also demonstrated this result in their study.

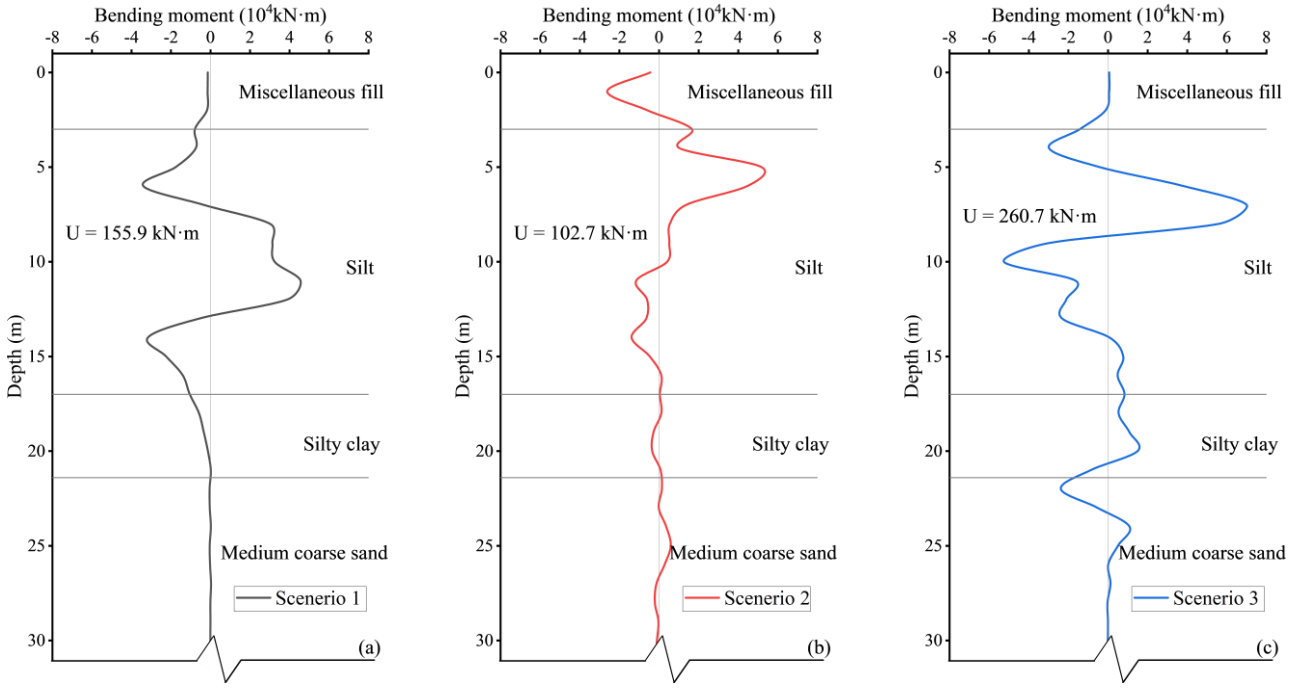


Fig. 4 Bending moment and strain energy of (a) scenario 1, (b) scenario 2 and (c) scenario 3

Among the scenarios analyzed, Scenario 3 exhibits the highest pile strain energy, followed by Scenario 1, while Scenario 2 shows the lowest pile strain energy. Compared with the work done on soil per linear meter discussed earlier, the pile strain energy differs significantly under similar work done on soil per linear meter in different scenarios (i.e. under similar horizontal displacement of bridge pier). This indicates that varying pile deflections result in different energy transfer efficiencies, meaning the ratio of work done on soil per linear meter to pile strain energy is not consistent across different scenarios.

## 5. Conclusions

This paper investigates the effects of grouting in silt-sand composite strata on the surrounding soil and bridge substructures. The interaction between grouting and bridge substructure behavior is analyzed using the work done on soil per linear meter as an intermediary variable. Based on the findings, three key conclusions are drawn:

- In this project, for a grouting distance range of [0, 5] (m) and a grouting volume range of [0, 120] ($m^3$), it can be assumed that the horizontal displacement of the bridge pier is directly proportional to the cumulative grouting volume.
- The relationship between the horizontal displacement of the bridge pier and the grouting volume can be divided into linear, nonlinear, and ineffective zones. For each grouting distance, there is a corresponding maximum horizontal displacement of the bridge pier. Beyond this point, any further increase in grouting volume will no longer result in additional displacement, marking the transition into the ineffective zone.
- The work done on soil per linear meter provides an overall response to the displacement effects at different soil depths. In the project addressed by this study, as an intermediate value, it effectively reflects the relationship between grouting and the bridge pier while also enabling real-time feedback on the horizontal displacement of the bridge pier under grouting conditions (Obtaining $k_2$ required).

The calculation of work done on soil per linear meter assumes that the soil between the inclinometer and the bridge pier is homogeneous and does not consider soil anisotropy. The soil is typically elastoplastic; however, in the model assumptions, the soil is treated as an elastic material with a constant elastic modulus, which does not adequately capture the soil's stress–strain behavior, leading to deviations in the calculated work done on soil per linear meter. These factors constitute potential sources of error and limitations of the proposed method. Future work will focus on further refining the model by incorporating the nonlinear behavior of the soil.

The proposed method demonstrates good applicability and accuracy under the geological conditions of the present project; however, its suitability under different stratigraphic conditions requires further investigation. This will also be a key focus of subsequent research.

## Acknowledgements

This research is funded by the Natural Science Foundation of Guangdong Province of China (Grant No. 2023A1515012084).

## References


Bayesteh, H. and Sabermahani, M. (2020), "Field study on performance of jet grouting in low water content clay", *Eng. Geol.*, **264**, 105314. https://doi.org/10.1016/j.enggeo.2019.105314.

Boschi, K., Di Prisco, C.G. and Ciantia, M.O. (2020), "Micromechanical investigation of grouting in soils", *Int. J. Solids Struct.*, **187**, 121-132. https://doi.org/10.1016/j.ijsolstr.2019.06.013.

Cao, L.F. (2001), "Undrained cavity expansion in modified Cam clay I: Theoretical analysis", *Géotechnique*, 323-334.

Cheng, S.H., Chao, K.C., Wong, R.K.N. and Wang, M.I.M. (2023), "Control of jet grouting process induced ground displacement in clayey soil", *Transp. Geotech.*, **40**, 100983. https://doi.org/10.1016/j.trgeo.2023.100983.

"Code for Design of Concrete Structures" (2010), Beijing, China.

El-Kelesh, A.M., Mossaad, M.E. and Basha, I.M. (2001), "Model of compaction grouting", *J. Geotech. Geoenviron. Eng.*, **127**, 955-964. https://doi.org/10.1061/(ASCE)1090-0241(2001)127:11(955).

Flora, A., Modoni, G., Lirer, S. and Croce, P. (2013), "The diameter of single, double and triple fluid jet grouting columns: Prediction method and field trial results", *Géotechnique*, **63**(11), 934-945. https://doi.org/10.1680/geot.12.P.062.

Fu, Y., Wang, B., Wu, H., Chen, X., Sun, X., Bian, Y. and Shen, X. (2023), "Theoretical analysis on horizontal rectification of tunnel near deep foundation pit by grouting", *Tunn. Undergr. Sp. Tech..*, **133**, 104977. https://doi.org/10.1016/j.tust.2022.104977.

Jaky, J. (1944), "The coefficient of earth pressure at rest. In Hungarian (A nyugalmi nyomas tenyezoje)", *J. Soc. Hungarian Archit. Eng.*, 355-358.

Jia, B., Gao, Z. and Hua, H. (2023), "Prediction method of soil horizontal displacement caused by non-uniform distribution of disturbance force in shield construction", *FACETS*, (Ed., Vlachopoulos, N.), **8**, 1-17. https://doi.org/10.1139/facets-2022-0197.

Kim, S.H., Jung, Y.H. and Shin, J.H. (2024), "Underground cavity remediation using membrane grouting method", *Geomech. Eng.*, **38**(5), 455–466. https://doi.org/10.12989/gae.2024.38.5.455.

Li, C., Lu, M., Zhu, B., Liu, C., Li, G.Y. and Mo, P.Q. (2024), "Analysis of cavity expansion based on general strength criterion and energy theory", *Geomech. Eng.*, **37**(1), 9-19. https://doi.org/10.12989/gae.2024.37.1.009.

Li, S., Deng, Z., Wei, L., Chen, Q., Zhang, Y. and He, F. (2025), "Lateral behavior of high-speed railway bridge pile foundation in soft soils under adjacent surcharge loads considering time-dependent characteristics", *Alexandria Eng. J.*, **110**, 451-467. https://doi.org/10.1016/j.aej.2024.10.044.

Liu, H., Zhou, H., Kong, G., Qin, H. and Zha, Y. (2017), "High pressure jet-grouting column installation effect in soft soil: Theoretical model and field application", *Comput. Geotech.*, **88**, 74-94. https://doi.org/10.1016/j.compgeo.2017.03.005.

Lu, C., Zhang, X., Shi, B., Jiang, J. and Lin, Z. (2024), "Deformation in settlement and grouting remediation of thickened larger-diameter metro shield tunnel in soft soil: A case study", *Case Stud. Constr. Mater.*, **20**, e02736. https://doi.org/10.1016/j.cscm.2023.e02736.

Ma, M., Yang, X., Zhou, J., Li, L. and Tian, J. (2024), "Model tests and numerical simulations of deformation repair effect for operating shield tunnels under horizontal lateral grouting", *Transp. Geotech.*, **47**, 101277. https://doi.org/10.1016/j.trgeo.2024.101277.

Milkevych, V., Munkholm, L.J., Chen, Y. and Nyord, T. (2018), "Modelling approach for soil displacement in tillage using discrete element method", *Soil Tillage Res.*, **183**, 60-71. https://doi.org/10.1016/j.still.2018.05.017.

Park, D. and Oh, J. (2018), "Permeation grouting for remediation of dam cores", *Eng. Geol.*, **233**, 63-75. https://doi.org/10.1016/j.enggeo.2017.12.011.

Sha, F., Zhang, L., Zhang, M., Zuo, Y. and Niu, H. (2024), "Penetration grouting diffusion and strengthening mechanism of sand layer with crucial grout", *J. Build. Eng.*, **91**, 109585. https://doi.org/10.1016/j.jobe.2024.109585.

Shan, Y., Luo, J., Wang, B., Zhou, S. and Zhang, B. (2024), "Critical application zone of the jet grouting piles in the vicinity of existing high-speed railway bridge in deep soft soils with medium sensibility", *Soils Found.*, **64**, 101407. https://doi.org/10.1016/j.sandf.2023.101407.

Shen, S.L., Wang, Z.F. and Cheng, W.C. (2017), "Estimation of lateral displacement induced by jet grouting in clayey soils", *Géotechnique*, **67**, 621-630. https://doi.org/10.1680/jgeot.16.P.159.

Sun, Y., Shen, S., Xu, Z. and Xia, X. (2014), "Prediction of lateral displacement of soil behind the reaction wall caused by pipe jacking operation," *Tunn. Undergr. Sp. Tech.*, **40**, 210-217. https://doi.org/10.1016/j.tust.2013.10.010.

Wang, C., Guo, C., Du, X., Shi, M., Liu, Q. and Xia, Y. (2021), "Reinforcement of silty soil with permeable polyurethane by penetration injection", *Constr. Build. Mater.*, **310**, 124829. https://doi.org/10.1016/j.conbuildmat.2021.124829.

Wang, L. and Zheng, G. (2024), "Numerical analysis of underground displacements stirred by compaction grouting during tunnel construction", *Tunn. Undergr. Sp. Tech.*, **152**, 105931. https://doi.org/10.1016/j.tust.2024.105931.

Wang, Z.F., Shen, S.L. and Modoni, G. (2019), "Enhancing discharge of spoil to mitigate disturbance induced by horizontal jet grouting in clayey soil: Theoretical model and application", *Comput. Geotech.*, **111**, 222-228. https://doi.org/10.1016/j.compgeo.2019.03.012.

Wu, Y., Diao, H., Liu, J. and Zeng, C. (2016), "Field studies of a technique to mitigate ground settlement of operating highways", *J. Zhejiang Univ. Sci. A*, **17**, 565-576. https://doi.org/10.1631/jzus.A1600231.

Xia, H., Du, G., Cai, J. and Sun, C. (2024), "Model tests on the bearing capacity of pervious concrete piles in silt and sand", *Geomech. Eng.*, **38**(1), 79–91. https://doi.org/10.12989/gae.2024.38.1.079.

Zhang, D., Ye, Z., Chu, W., Zhang, J. and Shao, H. (2024a), "Experimental study on the rehabilitation of a shield tunnel lining with excessive transverse deformation by lateral grouting," *Tunn. Undergr. Sp. Tech.*, **148**, 105748. https://doi.org/10.1016/j.tust.2024.105748.

Zhang, W., Li, Y., Goh, A.T.C. and Zhang, R. (2020), "Numerical study of the performance of jet grout piles for braced excavations in soft clay", *Comput. Geotech.*, **124**, 103631. https://doi.org/10.1016/j.compgeo.2020.103631.

Zhang, Y., Cao, Z., Liu, C. and Huang, H. (2024b), "Fluid-solid coupling numerical simulation of micro-disturbance grouting treatment for excessive deformation of shield tunnel", *Underground Sp.*, **19**, 87-100. https://doi.org/10.1016/j.undsp.2024.02.003.

Zhao, T. and Wang, Y. (2018), "Interpretation of pile lateral response from deflection measurement data: A compressive sampling-based method", *Soils Found.*, **58**(4), 957-971. https://doi.org/10.1016/j.sandf.2018.05.002.


*GC*